Journal of Electroceramics, 11, 149–155, 2003

The Synthesis and Composition of Dual-Phase 3Y-TZP/RuO_2 Electrode Powders

TOMAS P. RAMING,* WERNER E. VAN ZYL, RIAAN SCHMUHL & HENK VERWEIJ†

Laboratory for Inorganic Materials Science, Department of Chemical Technology and MESA+ Research Institute, University of Twente, P.O. Box 217, 7500 AE Enschede, The Netherlands

Submitted June 3, 2003; Revised December 3, 2003; Accepted January 9, 2004

Abstract. This research was performed to learn more about the electron conducting yttria doped zirconia/ruthenia dual-phase system. The study indicated that for all starting powder precipitates (by either co-precipitation or sequential precipitation) strong separation between the Ru and Zr-species upon heating occurred already at the unexpected low temperature of 100–200°C. The solubility of RuO_2 in 3Y-TZP (zirconia stabilised into a tetragonal phase by a 3 mol% Y_2O_3 addition) after calcination at 600°C was estimated at 3 mol%, independently of the used synthesis technique.

Keywords: composites, homogeneity, solid solubility, zirconia, ruthenia

Introduction

Ruthenia (RuO_2) is one of the very few single oxides that have electronic conduction as high as that of metals [1], which makes it interesting as electrode material. There are two major drawbacks for the use of ruthenia as electrode material, though: first, the high price of ruthenia in comparison with metals such as copper or nickel, and second, the large-scale reaction of RuO_2 with oxygen at temperatures above 700°C to form the volatile RuO_3 and RuO_4 [2].

An inert, low-cost oxide is often added to the ruthenia to reduce the costs and to stabilise the ruthenia phase without losing the metallic conduction (e.g. TiO_2 [3], or yttria-stabilised zirconia [4–6]). Recently it was shown that a dense, sintered compact with 85 mol% of yttria-stabilised-zirconia and 15 mol% of ruthenia still had metallic conduction [7].

The content of ruthenia phase in the dual-phase zirconia-ruthenia material might be even decreased to below 15 mol%, without losing the electronic conduction. The value of the percolation limit, as almost any other property of a zirconia-ruthenia composite, will not only depend on the proportions of the two phases, but will also be determined by the interaction between the two metal oxides, which can be divided up into several components.

The first component is the extent of the dissolution of the ruthenia phase into the zirconia phase, since it has been reported that ruthenia can dissolve into a zirconia phase up to a maximum value of 10 mol% [8–11]. The more ruthenia dissolves into the zirconia phase, the more ruthenia has to be added to create a percolative system.

A second important component is the microstructure of the composites. It has been shown that ruthenia-YSZ compacts show large-scale phase separation upon sintering at temperatures of 1000°C or higher [7], as a result of the aforementioned oxidation of ruthenia. It was shown that the powder preparation method (co-precipitation or sequential precipitation) has a large influence on the resulting microstructure and thus on the electrical properties of the final ceramic [7]. Therefore the relation between the powder precipitation method and the solid solubility of ruthenia into the zirconia phase as well as the spatial distribution of the two phases has been investigated.

*Correspondence address: Patentlaan 2, P.O. Box 5818, 2280 HV Rijswijk, The Netherlands. E-mail: traming@epo.org

†Present address: Department of Materials Science and Engineering, The Ohio State University, Columbus, OH 43210-1178, USA.

Experimental

Synthesis

The first type of powder synthesis used was a Co-Precipitation (CP). An aqueous solution of $ZrOCl_2 \cdot 8H_2O$ (Merck, Germany), YCl_3 (Cerac, USA) and $RuCl_3 \cdot 3.4H_2O$ (Acros, Belgium) with pH 2 and total metal ion concentration of 1.7–3.0 M was filtered through a 0.025 μm membrane. This solution was slowly (in 6 h) added through a tube into a concentrated aqueous ammonia (pH $\sim$ 14) solution, while stirring vigorously. By placing the narrow (1.5 mm inner diameter) insertion tube directly above the tip of the stirrer the amount of nucleation sites was maximised (and nucleus growth minimised). During the addition process, the gradual decrease in basicity was brought to a stop at a minimal pH of 12 through additions of ammonia. The resulting black gel was filtered and washed with distilled water to remove most chloride ions. Below pH 9 the precipitate was finally washed with ethanol until the density of the filtrate was below 0.79 g cm^{-3} (i.e. water content <5%). The black coloured gel, suspended in ethanol, was then oven-dried overnight at 100°C. The resulting amorphous powder was mortared and then calcined in air at different temperatures for 2 h at a heating rate of 2°C min^{-1}.

The second synthesis type, the Sequential Precipitation method (SP) encompassed first the synthesis of a zirconia gel, and subsequently the precipitation of a ruthenia salt in this gel. An aqueous solution which contained $ZrOCl_2 \cdot 8H_2O$ and YCl_3 was prepared and slowly added to aqueous ammonia (pH $\sim$ 14) using the same set-up as described for the CP method. The resulting gel was concentrated by filtration and subsequently subjected to hydrothermal treatment through heating in a closed vessel at 200°C under 10^6 Pa pressure for 2 h to form crystalline 3Y-TZP [12]. Then the gel was dispersed again in aqueous ammonia (pH $\sim$14) by vigorous stirring. An aqueous $RuCl_3 \cdot 3.4H_2O$ solution was slowly added to the 3Y-TZP suspension over 5 h, using again the aforementioned precipitation set-up. The further washing, drying and calcining procedure of the resulting mixed gel was as described above for the CP powders.

Single phase RuO_2 and 3Y-TZP powders were made as well, for comparison, by using the same precipitation set-up and procedure as in the case of the CP-powders. After separate calcination at 600°C, single phase ruthenia and 3Y-TZP powders were mixed at different proportions by using a mortar. The resulting zirconia-ruthenia composites are designated MX-powders.

Powder Characterisation

Quantitative X-ray fluorescence (XRF) was performed on a Philips PW 1480/10-fluorometer in order to determine the chemical compositions of the prepared powders [13].

For powder X-ray Diffraction (XRD) and X-ray Line Broadening (XRLB) a Philips X'Pert-1 PW3710 diffractometer was used. The same apparatus was used to measure the X-ray Line Broadening (XRLB) to determine the average crystallite size of the phases of the powders, thereby using the Scherrer formula [14].

Transmission electron microscopy (TEM) coupled with Energy Dispersive X-ray analysis (EDX) was performed with a Philips EM30 Twin/STEM TEM, provided with a KEVEX Delta-Plus EDX to determine the crystallites sizes and the chemical compositions at randomly selected spots within the powders. The spot diameter for EDX measurements in all cases was 34 nm.

The homogeneity of the distribution of the two phases in the powders was probed by performing a series of EDX measurements. First the powders were pressed uniaxially at 1000 MPa into 50–60% dense cylindrical compacts of 10 mm diameter and a few mm height. A Hitachi S800 (Japan) SEM, equipped with a Kevex Delta Energy *V* dispersive X-ray analysis system was used for EDX measurements on the carbon coated (5 nm layer) pressed powders. On each sample a series of EDX-measurements on 20 different spots was performed. Each measured (micro)locality had both a diameter and information depth of around 1 μm. The measured spots were chosen on the whole surface of each sample, but were not chosen totally at random. To avoid too much scattering of the electron bundle, pores and large particulates were avoided as much as possible.

The homogeneity *Ho* thus was quantified with the following formula:

$Ho = t_n(99) * (s/\mathrm{Ru_{av}})$, where $\mathrm{Ru_{av}}$ = average Ru-content, s = relative standard deviation and $t_n(99)$ = Student-factor (5,84) [15].

The aforementioned SEM-apparatus was also used to take SEM-pictures of the surface of the pressed powders.

Table 1. Quantitative XRF data (mol%) showing the elemental composition of the system Y_2O_3-doped-ZrO_2 and RuO_2 nanocomposite powders after calcination at 600°C.

Powder	RuO_2	ZrO_2	$YO_{1.5}$	HfO_2	Cl
CP46	46.3	49.7	3.1	0.5	0.1
CP33	33.0	63.0	3.2	0.6	0.2
CP15	15.1	79.4	4.1	1.0	0.3
CP9	9.3	85.0	4.7	1.1	
CP5	4.7	89.5	4.6	1.2	
SP35	34.8	61.4	2.7	0.6	0.4
SP10	9.6	84.5	4.8	1.1	
SP5	4.9	89.1	4.9	1.2	

Results

Composition of Calcined Powders

The elemental compositions of the powders after calcination at 600°C were determined by quantitative XRF. The results are shown in Table 1.

After calcination at 600°C all powders showed the same phases in the XRD-pattern, a mixture of RuO_2 and tetragonal and/or cubic zirconia. According to the XRLB-measurements the average crystal sizes for both phases of all powders was in the nanoscale domain (<20 nm). The zirconia crystallite size of all powders was around 10 nm, while the ruthenia crystals were around 20 nm for all powders.

All XRD-spectra of the calcined powders showed the presence of the (112) reflection at 42°2θ, which is specific for tetragonal zirconia [17], but that does not exclude the presence of cubic zirconia [18]. Therefore the exact position of the zirconia (111) reflection in all spectra was determined. For all powders this position was below 30.25°2θ, close to the 30.2°θ of *t*-zirconia [17], and more far away from the 30.5°2θ of *c*-zirconia [18]. This is a clear indication that the zirconia for the large majority at least was in the tetragonal phase.

The XRD-patterns were used to estimate the solubility of RuO_2 in yttria-doped-zirconia. The area of the 28°2θ (110) ruthenia reflection (Ar) was divided by the sum of the areas of the 28°2θ (110) ruthenia reflection (Ar) and the 30°2θ (111) zirconia-reflection (Az), for the MX, SP and CP-powders, as can be seen in Fig. 1. This value (Ar/(Ar + Az)) is taken as a measure for the amount of ruthenia phase present. For the MX powders it is assumed that no ruthenia was dissolved in the zirconia phase, since the two phases of this powder were prepared separately and the careful mixing by grinding unlikely could have caused phase mixing. Therefore the fitted line through the data points for the MX powders originated from the origin.

The fitted lines for the CP and SP powders are close to the fitted line for the MX powder, indicating that only a small amount of around 3 mol% RuO_2 has been dissolved into the zirconia phase of the SP5 and CP5 powders. The amount of dissolved ruthenia into the zirconia phase decreases when increasing the amount of ruthenia present in the composites, especially for the CP powders.

Morphology and Homogeneity of the Powders

In Fig. 2 a TEM-picture of the CP5 powder is shown. The individual crystals are clearly visible. It was not

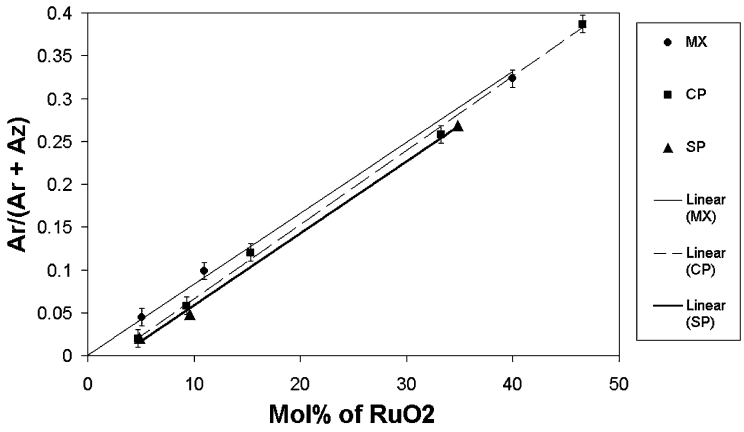

Fig. 1. The area of the ruthenia-reflection in the XRD-diagram (Ar) divided by the area of the zirconia-reflection in the same XRD-diagram (Az) and Ar, as calculated for the different CP, SP and MX powders.

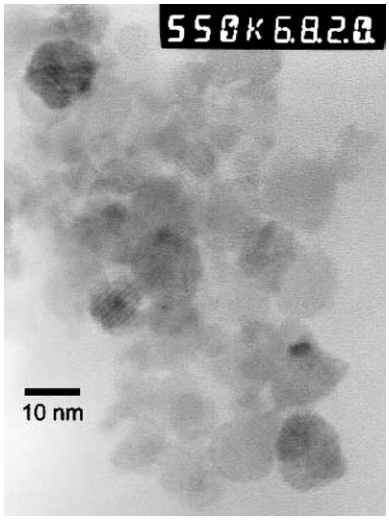

Fig. 2. TEM-picture of the CP5 powder calcined at 600°C.

possible to identify the zirconia and ruthenia crystals separately with TEM at this spot; they were too small, as was already indicated by XRLB. When measuring the chemical composition at different places in the powders with TEM/EDX, it was often very deviating from the average composition. Since also some very large ruthenia crystals were detected with TEM, the ruthenia-zirconia powders were pressed into green compacts, which were further investigated with SEM.

Figure 3 shows a pressed compact of CP33 powder (calcined at 600°C). Ruthenia particulates (identified with EDX) of several micrometers are visible. These large ruthenia particulates were also visible in the pressed compacts of the other calcined CP-powders and SP-powders (see Fig. 4). Individual zirconia crystallites or clusters could not be identified with SEM/EDX. The smaller ruthenia particulates (50–100 nm) were incorporated into the homogeneous matrix while the larger ruthenia particulates were usually surrounded by large pores. The pressed compacts of the uncalcined CP-powders did not show any of these large ruthenia particulates. The lowest calcination temperature at which the large "RuO_2" particulates were observed with SEM was 400°C.

This inhomogeneity in the distribution of the zirconia and ruthenia phases was investigated more thoroughly with SEM/EDX, as already explained in the experimental part. The homogeneity is indicated by the parameter *Ho;* the higher its value, the more inhomogeneous the distribution of the two elements Ru and Zr within the powder. As can be seen from Fig. 5, the value of *Ho* for powder CP33 increases exponentially with calcination temperature, at least up to the highest calcination temperature of 700°C, which means that the chemical homogeneity (between the Zr and Ru elements) decreases rapidly with increasing calcination temperature. For the other CP-powders the same effect was observed, as well as for the SP-powders. Figure 5 also indicates that the zirconia and ruthenia phases were more homogeneously distributed in the CP-powders compared to the SP-powders.

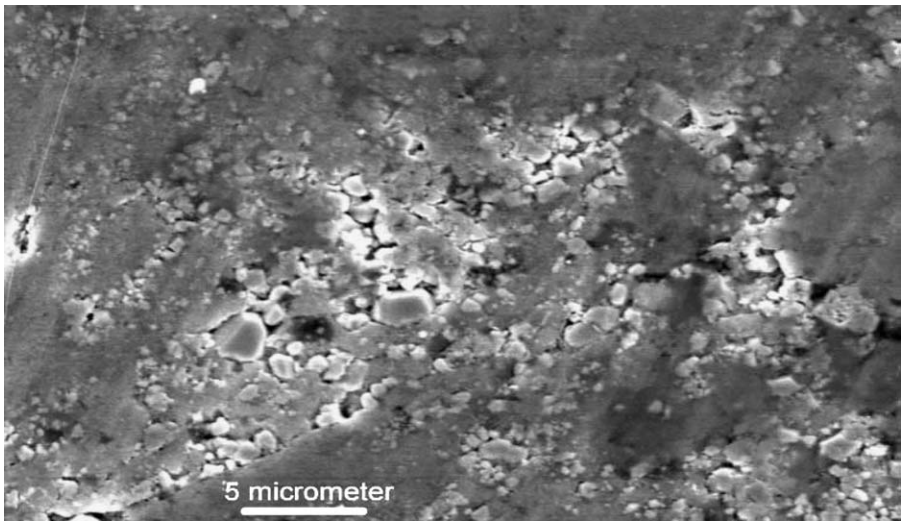

Fig. 3. SEM photo CP33 composite powder (calcined at 600°) pressed into a green compact.

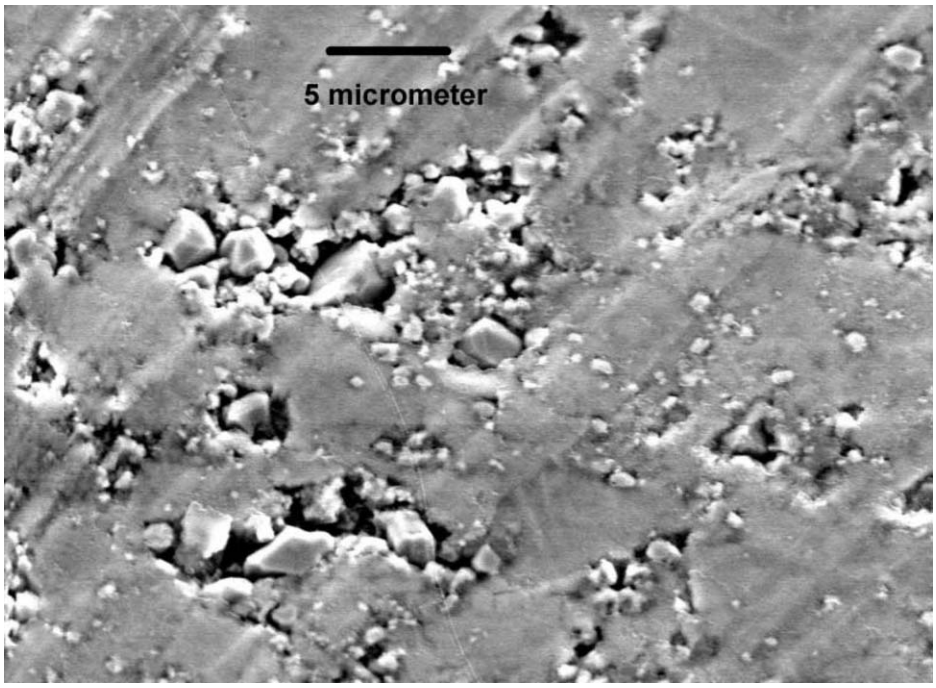

Fig. 4. SEM photo of SP35 composite powder (calcined at 600°) pressed into a green compact.

Discussion

Colomer and Jurado reported a solubility (detected by XRD) of RuO_2 in ZrO_2 of 8–10 mol% at temperatures up to 500°C for the amorphous solid-state solution $[(ZrO_2)_{0.92}(Y_2O_3)_{0.08}]_{1-x}(RuO_2)_x (0 \leq x \leq 0.3$ mole), obtained by a sol-gel process [8, 9]. Djurado et al. found the solubility of RuO_2 in ZrO_2 (by XRD) to be 10–12.5 mol% for the related amorphous system $[(ZrO_2)_{0.91}(Y_2O_3)_{0.09}]_{1-x}(RuO_2)_x$ ($0 \leq x \leq 0.2$ mole), which was made by drying the metal nitrate salts and subsequent calcination at 900°C [10]. Long et al. [11]

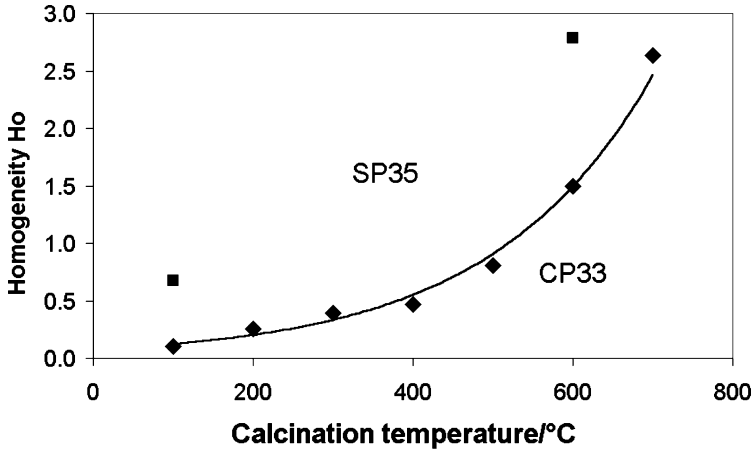

Fig. 5. Homogeneity of CP33 (diamonds) and SP35 (squares) as a function of calcination temperature.

used the same synthesis route as Djurado but found a solubility limit of 10–15 mol% up to 800°C (by XRD) for the system $[(ZrO_2)_{1-x}(RuO_2)_x]$ ($0 \leq x \leq 0.15$ mole). Thus, the results of Colomer [8, 9], Djurado [10] and Long [11] are in good agreement with each other and indicate a solubility of ca. 10% RuO_2 in both undoped ZrO_2 and yttria stabilised ZrO_2 when using the co-precipitation method.

Comninellis [19], however, reported that no mixed-phase exists in the RuO_2-ZrO_2 system. The conclusion was based on XRD data obtained from the precipitation of mixed solutions of aqueous $RuCl_3$ and $ZrOCl_2$ that were calcined at 460°C [19].

The results of this investigation are most in alignment with the results of Comninellis [19], since it can be concluded from Fig. 1 that the solubility of RuO_2 in YSZ is not more than 3 mol%. The assumption that the ruthenia of the MX-powders did not dissolve into the zirconia phase as a result of the grinding together of the two powders is confirmed by reports that state that heating a composite obtained from dry powder mixing of RuO_2 and ZrO_2 powders does not lead to dissolution of one oxidic phase into the other [6, 20].

The explanation of the difference between this low solubility limit and the higher solubility limits of around 10 mol% RuO_2 reported by others, may be connected with differences in the used synthesis methods for the zirconia-ruthenia powders. One striking difference is that both the zirconia-ruthenia powders reported here and the zirconia-ruthenia powders reported by Comninellis were made from chloride salts. The zirconia-ruthenia powder systems that were reported to have a solubility limit for ruthenia in zirconia of around 10 mol% were made from non-halogenated precursors [8–11], mostly nitrate precursors [10, 11]. As Table 1 shows, even though the precipitates were thoroughly washed, the calcined powders still contained a small amount (0.1–0.4 mol%) of chloride, which might have caused a different amorphous structure for the precipitated powders, influencing the phase formation process during calcination.

The SEM/EDX measurements made clear that the as-precipitated, amorphous CP powders had a highly homogeneous distribution of the metal ions Zr and Ru, while the SP method, as expected led to a less homogeneous distribution of the two elements (see Fig. 5). More remarkable, however, is the strong dehomogenisation between the zirconia and ruthenia phases for all powders that increases with increasing calcination temperature. Strictly speaking, the homogeneity that was measured is the homogeneity of the distribution of the two elements Ru and Zr. Regarding the low solubility of RuO_2 in the YSZ-phase, this homogeneity can just as well be regarded as the homogeneity of the distribution of the two phases ruthenia and YSZ.

Figure 5 shows that this segregation already started below 200°C. The segregation also indicates a very low solubility of ruthenia in YSZ, in agreement with the XRD results obtained. Segregation of Zr and Ru at a low temperature has been observed before in a mixed zirconia/ruthenia film calcined at 400°C [4]. It has been observed that there is a strong driving force for segregation of ruthenia to the pores from many oxides (TiO_2 [21, 22], SnO_2 [23] and VO_3 [24].) at relatively low temperatures (400–600°C), however it has not been reported before that this segregation already starts below 200°C, as is reported here. Colomer and Jurado [25] suggested that the segregation effect is indicative of RuO_2 oxidation, starting at a much lower temperature than the 800°C reported by Tagirov [2]. The small crystallite size of the ruthenia crystals and consequent high surface area may enhance the rate of oxidation processes dramatically, which accelerates the formation of volatile RuO_3 and/or RuO_4 type species [2]. This is also indicated by the fact that the nanocrystalline ruthenia phase of all powders totally evaporated when heating above 700°C, instead of above 800°C.

It is very likely that the electrical conductivity of the compacts that can be made from the here described powders will be influenced by the used powder calcination temperature. The higher the calcination temperature, the more the ruthenia has moved together to form separated ruthenia agglomerates. This could improve the electrical conductivity of the ceramics and lower the percolation limit to below the reported 15 mol%, by compacting zirconia-ruthenia powders with 5–15 mole% ruthenia. The fact that the solubility of the ruthenia into the zirconia phase is quite small also is advantageous when trying to lower the percolation limit. The calcination temperature should not be taken higher than 700°C though, since this will lead to loss of ruthenia from the powder.

Conclusions

Formation of a dual-phase powder consisting of yttria-doped-tetragonal zirconia and ruthenia has been achieved through calcination of co-precipitated (CP) and sequentially precipitated (SP) powders. The

precipitation of a solution containing the appropriate metal species in aqueous ammonia (pH 12–14) led to an amorphous and very homogeneous powder on a scale of 1 μm for the co-precipitation method. The precipitation of amorphous ruthenia into a gel of crystalline zirconia (sequential precipitation) conceived a less homogeneous distribution of the two components.

When heating the precipitated fully amorphous CP-powders and partially amorphous SP-powders the (at the beginning hydrous) ruthenia and zirconia started immediately to separate from each other, as was shown by EDX-research. The strong separation of ruthenia from other oxides (such as zirconia) into micron sized ruthenia aggregates has been reported before to start at a temperature of 400°C, but the here performed EDX-research made it possible to show that this segregation already starts at the very low temperature of $<$200°C. The homogeneity of the zirconia-ruthenia distribution decreased exponentially with increasing temperature.

The solubility of RuO_2 in 3Y-TZP was estimated (by XRD) to be between around 3 mol% for both the co-precipitated and sequentially precipitated powders prepared from chloride precursors and calcined at 600°C, in the case low amounts of ruthenia were added ($<$10 mol%). With increasing ruthenia addition the dissolution of the ruthenia into the zirconia decreased.

Acknowledgments

Dr. Stein from the Max-Planck Institute in Düsseldorf is thanked for performing the DSC-measurements, M. Smithers for the TEM and SEM/EDX measurements and H. Koster for the XRD measurements. We gratefully acknowledge the Netherlands Organisation for Scientific Research (NWO), group of Chemical Sciences (CW) for financial support.

References

1. J.B. Goodenough, *Prog. Solid State Chem.*, **5**, 145 (1971).
2. V.K. Tagirov, D.M. Chizhikov, E.K. Kazenas, and L.K. Shubochkin, *Rus. J. Inorg. Chem.*, **20**, 1133 (1975).
3. W.A. Gerrard and B.C.H. Steele, *J. Appl. Electrochem.*, **8**, 417 (1978).
4. O.R. Camara and S. Trasatti, *Electrochim. Act.*, **41**, 419 (1996).
5. L.D. Burke and M. McCarthy, *Electrochim. Act.*, **29**, 211 (1984).
6. M. Hrovat, J. Holc, and D. Kolar, *Solid State Ion.*, **68**, 99 (1994).
7. T.P. Raming, W.E. van Zyl, and H. Verweij, *Chem. Mat.*, **13**, 284 (2001).
8. M.T. Colomer and J.R. Jurado, *J. Solid State Chem.*, **141**, 282 (1998).
9. M.T. Colomer and J.R. Jurado, *J. Non-Cryst. Solids*, **217**, 48 (1997).
10. E. Djurado, C. Roux, and A. Hammou, *J. Eur. Ceram. Soc.*, **16**, 767 (1996).
11. Y.C. Long, Z.D. Zhang, K. Dwight, and A. Wold, *Mater. Res. Bull.*, **23**, 631 (1988).
12. C.D. Sagel-Ransijn, A.J.A. Winnubst, A.J. Burggraaf, and H. Verweij, *J. Eur. Ceram. Soc.*, **16**, 759 (1996).
13. M. Bos, J.A.M. Vrielink, and W.E. van der Linden, *Anal. Chim. Act.*, **412**, 203 (2000).
14. P. Scherrer, *Goett. Nachr.*, **2**, 98 (1918).
15. J.S. Fritz and G.H. Schenk, in *Quantitative Analytical Chemistry,* edited by Allyn and Bacon (Boston, USA, 1974).
16. JCPDS-International Centre for Diffraction Data, #04-0802.
17. JCPDS-International Centre for Diffraction Data, #17-0923.
18. JCPDS-International Centre for Diffraction Data, #27-0997.
19. Comninellis and G.P. Vercesi, *J. Appl. Electrochem.*, **21**, 335 (1991).
20. M. Hrovat, S. Bernik, and J. Holc, *J. Mater. Sci. Lett.*, **18**, 1019 (1999).
21. K. Kameyama, S. Shohji, S. Onoue, K. Nishimura, K. Yahikozawa, and Y. Takasu, *J. Electrochem. Soc.*, **140**, 1034 (1993).
22. Y. Takasu, S. Onoue, K. Kameyama, Y. Murakami, and K. Yahikozawa, *Electrochim. Acta*, **39**, 1993 (1994).
23. M. Ito, Y. Murakami, H. Kaji, K. Yahikozawa, and Y. Takasu, *J. Electrochem. Soc.*, **143**, 32 (1996).
24. Y. Takasu, T. Nakamura, H. Ohkawauchi, and Y. Murakami, *J. Electrochem. Soc.*, **144**, 2601 (1997).
25. M.T. Colomer and J.R. Jurado, *Chem. Mater.*, **12**, 923 (2000).